SCIENTIFIC PAPERS
OF THE UNIVERSITY OF PARDUBICE
Series A
Faculty of Chemical Technology
17 (2011)

KINETIC PROCESSES IN Se-Te GLASSES

Roman SVOBODA[a1], Pavla HONCOVÁ[b] and Jiří MÁLEK[a]
[a]Department of Physical Chemistry,
[b]Department of Inorganic Technology,
The University of Pardubice, CZ–532 10 Pardubice,

Received September 13, 2011

Structural relaxation kinetics and crystallization kinetics of chosen compositions from the Se-Te glassy system were studied under non-isothermal conditions by using differential scanning calorimetry in dependence on particle size. The purpose of this contribution is to demonstrate the extent of information accessible by the present-day kinetic analysis provided by the differential scanning calorimetry and to suggest its importance and merit for the development of new high-tech PCM materials. Enthalpic relaxation was described on the basis of Tool–Narayanaswamy–Moynihan model. Single set of TNM parameters was obtained from the curve-fitting procedure for each studied glass. A comparison with our previous measurements on a-Se was made and the development of particular TNM parameters with increasing Te content was discussed in terms of changes in molecular structure of the material. The curve-fitting results were further verified by several independent non-fitting methods. The crystallization kinetics was described in terms of the nucleation-growth Johnson–Mehl–Avrami model. Complexity of the crystallization process was in this case represented by very closely overlapping consecutive competing surface and bulk nucleation-

[1] To whom correspondence should be addressed.

growth mechanisms. Mutual interactions of both mechanisms as well as all other observed effects were explained in terms of thermal gradients, surface crystallization centres arising from the sample preparation treatments and changing amount of volume nuclei originating from the combination of pre-nucleation period and the very glass preparation phase. Advanced error analysis was performed for each step of the kinetic study. A new criterion for quick determination of the dominating crystallization mechanism — surface or bulk — was introduced.

Introduction

Continually increasing interest in chalcogenide glasses results from their unique physical properties as, e.g., great distinction of amorphous and crystalline states by means of their reflectivity or electrical conductivity, numerous photoconductive effects or high transmittance in near, middle and far infrared region. Most important applications of chalcogenide glasses then involve large capacity data-storage media [1] (i.e., non-volatile PCRAMs where data are written via electric pulses or optically recorded CDs, DVDs and BlueRay Discs), sophisticated devices and elements for infrared optics and optoelectronics (fibers, planar guides, lenses) or various electronic thresholds and memory switches.

It is obvious that quality of the prepared glasses (or their thin layers) and their stability are the key factors for utilization in the high-tech applications. In this regard two physical processes occurring in glassy material have to be considered — structural relaxation and cold crystallization. Considering the structural relaxation, the applicability of chalcogenide glasses may be influenced by the changes in important physical properties accompanying the structural changes in consequence of the relaxation processes. In a similar way also the crystallization process can be limiting for the applicability of a newly developed glass. Crystallization has to be either avoided in order to obtain perfect and stable glass with finest optical or electrical properties or, on the contrary, the crystallization process in glassy matrix is in fact the fundamental basis of the technology — this is the case of data-storage media. Nevertheless, in either case it would appear to be extremely important to know precise mechanisms of nucleation and crystallization processes.

However, current approach to the development of new modern PCM materials for the hi-tech applications is rather empirical, and exact kinetics of the occurring basal processes is rarely known. In our opinion, it is the deeper understanding of important (and application-relevant) processes proceeding in these materials that will be essential for their further development and search for new application possibilities.

The purpose of this work is to summarize and demonstrate the extent of

information accessible by the present-day kinetic analysis provided by the differential scanning calorimetry and to suggest its importance and merit for the development of new high-tech materials.

The Se-Te glassy system (particularly glasses with compositions $Se_{90}Te_{10}$, $Se_{80}Te_{20}$ and $Se_{70}Te_{30}$) was chosen for multiple reasons. Selenium based chalcogenide glasses have gained much importance in the last few decades due to their numerous potential applications. However, from technological perspective, pure glassy selenium has considerable shortcomings (short lifetime, low photosensitivity and thermal instability) and certain additives are commonly used to overcome these limitations. It has been pointed out recently that selenium-tellurium alloys exhibit some advantages in comparison with pure a-Se, i.e. greater hardness, higher conductivity and photosensitivity, higher crystallization temperature and lower ageing effects [1-3]. The Se-Te system was, however, chosen not only for its technological potential (suitable matrix for numerous "hi-tech" applications) but also for its atypical thermal and structural behaviour interesting purely from the scientific point of view.

Theory

Structural Relaxation

Despite the great importance of non-crystalline materials and long history of their examination, the very process of glass forming is still not fully understood and the true nature of the glass transition phenomenon remains unrecognized.

Glass transition is a widely studied phenomenon that can be shortly described as a process at which some macroscopic property (volume, enthalpy, refraction index …) departs during continuing cooling from the undercooled liquid equilibrium state. The slope of the property-temperature curve decreases from its undercooled liquid value (higher temperature) to the glassy value (lower temperature). At that moment the glass is formed and the glass transition temperature T_g can be evaluated as an intersection of the liquid and glassy asymptotes. The non-equilibrium nature of the glassy state results in structural relaxation. This process occurs within and below the glass transition region and can be described as a spontaneous change of the structure towards its equilibrium state represented by the undercooled liquid extrapolation to the given temperature (Fig. 1). The rate at which the system approaches the equilibrium depends on actual temperature and structure (i.e., thermal history) of the glass [4].

During past decades a significant effort was put into development of various theoretical models describing the relaxation behaviour. Nowadays it is probably the phenomenological four-parameter Tool–Narayanaswamy–Moynihan (TNM) mo-

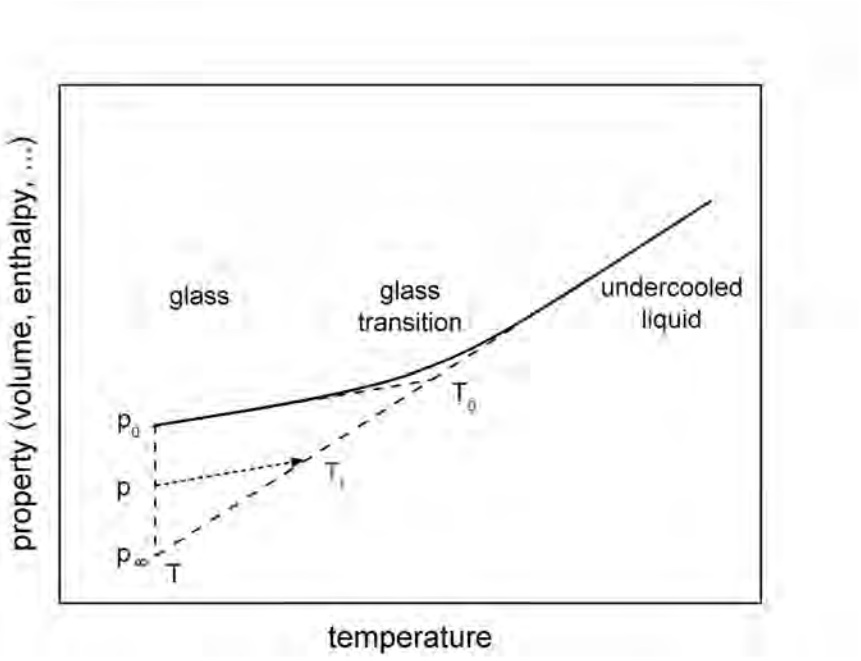

Fig. 1 Temperature dependence of a property (volume or enthalpy) relaxing at constant pressure. Index "0" represents initial state of the formed glass while index "∞" represents the equilibrium state of the material. Evaluation of the fictive temperature T_f is demonstrated

del based on Tool's concept of "fictive temperature" [5] that is being used most frequently. The model is represented by the following two equations.

It is a well known fact that structural relaxation is a non-exponential and non-linear process. Non-exponentiality of the structural relaxation is often described by means of the distribution of relaxation times which is expressed by the Kohlrausch–Williams–Watts (KWW) stretched exponential function [6,7]. The KWW function is defined as follows

$$\Phi(t) = \exp\left(-\xi^{\beta}\right) = \exp\left[-\left(\int_0^t \frac{\mathrm{d}t}{\tau}\right)^{\beta}\right] \tag{1}$$

where $\Phi(t)$ is the relaxation function, ξ is the reduced time, τ is the relaxation time which is a function of the temperature T and actual structure of the material, β is the parameter of non-exponentiality and is inversely related to the width of the relaxation times distribution ($0 \le \beta \le 1$).

The non-linear character of the structural relaxation is often described on the basis of Tool's concept [5] that the relaxation time depends on both temperature and actual structure of the material. This instantaneous structure of the system can be described by the fictive temperature T_f introduced by Tool. The fictive temperature is defined as the temperature of the undercooled liquid which has the same structure as the relaxing glass (Fig. 1). The concept of Tool was then modified by Narayanaswamy and Moynihan [8,9]

$$\tau(T, T_f) = A_{TNM} \exp\left[\frac{x\Delta h^*}{RT} + \frac{(1-x)\Delta h^*}{RT_f}\right] \tag{2}$$

where A_{TNM} is the preexponential factor (which stands for the relaxation time at an infinitely high temperature), x is the parameter of non-linearity which describes the temperature/structure ratio of contribution to the relaxation time, $\Delta h^*/R$ is the apparent activation energy of structural relaxation, the meaning of other symbols is obvious or explained above.

Evaluation of the TNM parameters is standardly done by curve-fitting. In our work the fitting was programmed on the basis of the following two equations [10], where the fictive temperature is determined on the basis of the Boltzmann superposition integral over time that can be also replaced by a corresponding integral over temperature

$$T_{f,n} = T_0 + \int_{j=1}^{n} \Delta T_j \left\{1 - \exp\left[-\left(\sum_{k=j}^{n} \Delta T_k / Q_k \tau_k\right)^{\beta}\right]\right\} \tag{3}$$

$$T_{f,n} = T_0 + \int_{j=1}^{n_A} \Delta T_j \left\{1 - \exp\left[-\left(\sum_{k=n_A}^{n} \Delta t_{e,k} / Q_k \tau_k\right)^{\beta}\right]\right\} \tag{4}$$

where T_0 is the initial equilibrium temperature and t_e is the annealing time; Eq. (3) applies to non-isothermal steps and Eq. (4) is used in the case of isothermal segments. The input data are introduced in the form of normalized heat capacity C_p^N

$$C_p^N = \frac{\mathrm{d}T_f}{\mathrm{d}T} = \frac{C_p - C_{pg}}{C_{pl} - C_{pg}} \tag{5}$$

The parameters of the TNM model were then obtained through a non-linear optimization method by using the Levenberg–Marquardt algorithm. Minimum of the residual sum of squares RSS was sought in order to obtain the best fit.

Alternatively, the TNM parameters can be obtained/verified with the use of various non-fitting methods based on the simple data analysis. Certain frequently used non-fitting methods are presented in the following text.

The apparent activation energy of structural relaxation Δh^* can be determined from the dependence of T_g on cooling rate. An equation derived by Ritland [11] for the relation of the cooling rate and fictive temperature for glasses without memory effects was later extended by Moynihan *et al*. [9] for systems that exhibit a spectrum of relaxation times. Assuming the concept of thermorheological

simplicity, i.e., that the distribution of relaxation times is temperature independent, the fictive temperature T_f, obtained when a glass is cooled through the glass transition region, is shown [9] to be related to the cooling rate q^- by

$$\frac{\mathrm{d}\ln|q^-|}{\mathrm{d}(1/T_f)} = -\frac{\Delta h^*}{R} \tag{6}$$

where the fictive temperature T_f corresponds to the conventional T_g value obtained on cooling, i.e., to the temperature of intersection of the extrapolated liquid and glass property-T curves. The structure of the glass achieved during the previous thermal history (represented by T_f) can be evaluated using the "equal area method" [9,12]. This method is based on the following equation

$$\int_{T^*}^{T_f} (C_{pl} - C_{pg})\,\mathrm{d}T_f = \int_{T^*}^{T'} (C_{pl} - C_{pg})\,\mathrm{d}T \tag{7}$$

where T^* is any temperature above T_g at which the heat capacity is equal to the equilibrium undercooled liquid value C_{pl} and T' is a temperature well below T_g where a constant glassy value of C_{pg} was achieved. In order to evaluate $\Delta h^*/R$ from three-step measurements, various cooling rates together with constant heating rate have to be applied.

Second non-fitting method for determination of Δh^* is based on the peak-shift method [13,14]. It was shown [15] that the apparent activation energy of structural relaxation can be evaluated from three-step DSC experiments where the ratio of the cooling and heating rates remains the same (i.e., the heating rate is not constant as it was in similar experiments mentioned in the previous paragraph but changes correspondingly with cooling rate). The evaluation can be performed according to the following equation

$$-\frac{\Delta h^*}{R} = \left[\frac{\mathrm{d}\ln|q^+|}{\mathrm{d}(1/T_p)}\right]_{q^-/q^+ = const} \tag{8}$$

where T_p is the temperature of the maximum of the endothermic relaxation peak.

Cold Crystallization

The crystallization process in glassy materials invoked by heating the glassy matrix is usually denoted as the so called "cold crystallization" in order for it to be distinguished from the "ordinary" crystal growth taking place in slowly cooled

liquid. Crystallization kinetics in glasses is very often studied by differential scanning calorimetry, DSC. The kinetic equation of DSC crystallization peak can be described [16] as

$$\Phi = \Delta H A e^{-\frac{E}{RT}} f(\alpha) \tag{9}$$

where Φ is the measured heat flow, ΔH is the crystallization enthalpy, A is the pre-exponential factor, E is the apparent activation energy of the process, R is the universal gas constant, T is temperature and $f(\alpha)$ stands for an expression of a kinetic model with α being conversion.

In order to describe the crystallization process by means of full kinetic analysis, Eq. (9) has to be evaluated. As the question of correct ΔH determination will be discussed in Experimental part, the first step of the kinetic analysis discussed within the framework of Theoretical section will be calculation of apparent activation energy of crystallization. There are numerous methods to calculate the activation energy E, however, probably the two most commonly and often used are the Kissinger [17] and Friedman [18] methods.

The method by Kissinger is applicable only under non-isothermal conditions and is based on the shift of the maximum of the crystallization peak T_p with heating rate q^+ according to the following equation

$$\ln \frac{T_p^2}{q^+} = -\frac{E}{RT_p} + const. \tag{10}$$

This method is based on an assumption that the conversion degree α corresponding to the maximum crystallization rate is constant and independent of experimental conditions. This assumption, on the other hand, is in fact the fundamental essence of Friedman's isoconversional method. In this method the apparent activation energy is calculated for various degrees of conversion according to the following equation

$$\ln \Phi_\alpha = -\frac{E}{RT_\alpha} + const \tag{11}$$

where Φ_α and T_α are the specific heat flow and temperature corresponding to certain chosen value of conversion α. The experimental data are here obtained again from crystallization curves measured at different heating rates and are plotted for each value of α separately. In this way eventually the dependence of activation energy E on the degree of conversion α is obtained. Due to the large influence of experimental conditions on the data quality of the crystallization peak tails, it is a common practice to consider only the values of E obtained for the interval $\alpha = 0.3$-0.7 when calculating average value. In an ideal case of a single and simple

crystallization process, the apparent activation energy should be independent of the degree of conversion α.

The second step of the kinetic analysis consist of choosing an appropriate kinetic model for the description of crystallization peaks. For this procedure Málek [19,20] suggested an algorithm based on the shape of characteristic functions $z(\alpha)$ and $y(\alpha)$. These functions are obtained by a very simple transformation of experimental data, for non-isothermal conditions the characteristic functions are defined as follows

$$y(\alpha) = \Phi e^{\frac{E}{RT}} \tag{12}$$

$$z(\alpha) = \Phi T^2 \tag{13}$$

The introduced functions are in fact a universal way for determination of an appropriate kinetic model applicable to any physical process. Determination of the most suitable kinetic model then utilizes both, values of α corresponding to the maxima of the characteristic functions and the overall shape of the functions. Based on this information, the optimal kinetic model can be chosen according to the algorithm [20] shown in Fig. 2 (where concrete values for several most common kinetic models are shown as well).

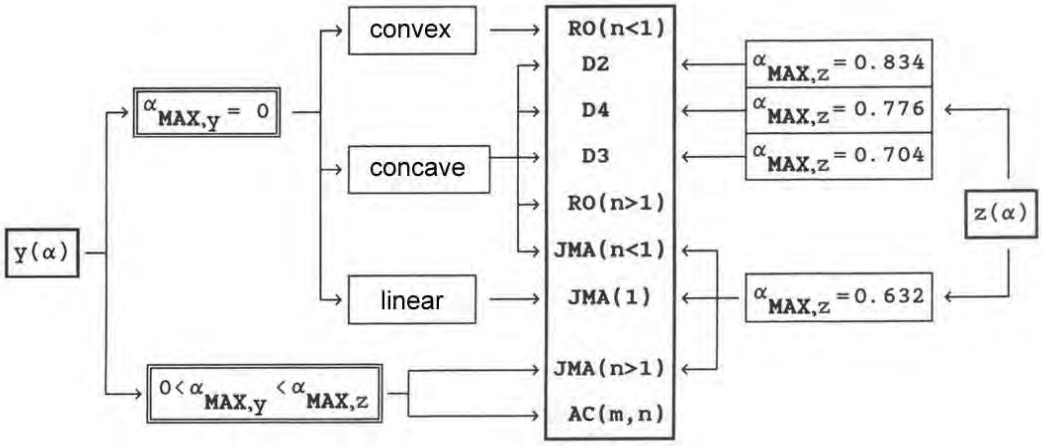

Fig. 2 Algorithm for determination of appropriate kinetic model based on values of maxima of $y(\alpha)$ and $z(\alpha)$ functions

In this work the two probably most popular and widely used kinetic models for description of the crystallization behaviour will be mentioned – the nucleation-growth Johnson–Mehl–Avrami (JMA) model and the autocatalytic Šesták–Berggren (AC) model. JMA(m) model [21-23] is a one-parameter model and its fundamental derivation has an actual physical basis. It can be expressed through the following equation

$$f(\alpha) = m(1-\alpha)\left[-\ln(1-\alpha)\right]^{1-(1/m)} \tag{14}$$

where m is the parameter reflecting nucleation and crystal growth mechanisms, as well as the crystal morphology. Equation (14) was derived strictly for isothermal conditions with additional assumptions being: the growth rate of a newly formed phase is controlled only by temperature and is independent of time and previous thermal history; nucleation is either homogeneous or heterogeneous on randomly distributed active centers; and growing crystals have low anisotropy. Nevertheless, Henderson [24,25] showed that the validity of this model can be extended also to non-isothermal conditions. This extension may be done under an assumption that the entire nucleation process takes place during early stages of the transformation and becomes negligible afterwards during the very crystal growth.

The crystallization kinetics following the JMA equation can be assumed when the value of degree of conversion corresponding to the maximum of the $z(\alpha)$ function $\alpha_{max,z}$ equals 0.632, which is the so-called "fingerprint" of the JMA model (see Fig. 2). Value of the kinetic parameter m itself can then be calculated from the conversion corresponding to the maximum of the $y(\alpha)$ function $\alpha_{max,y}$ according to [26]

$$m = \frac{1}{1+\ln(1-\alpha_{max,y})} \tag{15}$$

Alternative way of the parameter m determination is through double logarithm function [16]

$$\frac{d\ln\left[-\ln(1-\alpha)\right]}{d(1/T)} = -\frac{mE}{R} \tag{16}$$

In addition, linear dependence of this equation is also often considered a satisfactory condition for applicability of JMA model. Such condition, however, is not always justified [27].

The second model discussed within the framework of this article will be the autocatalytic AC(M, N) model [28]. This model is empirical, i.e., the model itself or its parameters do not have any physical basis or meaning, the description is purely phenomenological. AC model can be expressed through the following equation

$$f(\alpha) = \alpha^{M}(1-\alpha)^{N} \tag{17}$$

According to the algorithm shown in Fig. 2 it can be stated that, except for general boundary condition [29], the only condition for applicability of the AC model is the value of $\alpha_{max,y}$ being lower than $\alpha_{max,z}$, which is fulfilled practically for any

experimental data. Therefore, it is a usual and obvious practice to check the applicability of the physically meaningful JMA model first, and only in the case, when JMA equation cannot be used, the empirical AC model is applied.

Experimental

The set of studied chalcogenide glasses ($Se_{90}Te_{10}$, $Se_{80}Te_{20}$ and $Se_{70}Te_{30}$) was prepared from pure elements (5N, Sigma Aldrich) by the classical melt-quenching technique. Corresponding amounts of elements were accurately weighed into a fused silica ampoule, degassed and sealed afterwards. Total mass of each batch was approximately 10 g. The batched ampoule was then annealed in the rocking furnace at 650 °C for 24 hours. The glass was prepared from its melts by quenching the ampoule in water. The amorphous nature of the glass was checked by X-ray diffraction, homogeneity of the glass was verified from the position of the relaxation peak at T_g, which was measured under defined thermal history for samples taken randomly from the bulk glass. Relaxation and crystallization behaviours of the prepared glasses were studied using a conventional DSC 822^e (Mettler, Toledo) equipped with cooling accessory. Dry nitrogen was used as the purge gas at a rate of 20 cm^3 min^{-1}. The calorimeter was calibrated through the use of melting temperatures of In, Zn and Ga. The baseline was checked daily.

In our work we would like to show that careful experimental treatment together with its individual adaptation to the respective research intention may allow deriving of extra information about the studied objective. Particularly, in this publication we would like to emphasize the importance of particle size distribution study on the relaxation/crystallization kinetics.

Structural Relaxation

Regarding the structural relaxation measurements, perfect overall reproducibility of experimental conditions is the key factor. The reason for this subsists in the fact that the T_g relaxation overshoot itself is a relatively small thermal effect and, moreover, in order to study relaxation even subtle changes in the height, shape and position of this peak play vital role and have to be recognized. In this regard, each instability of the instrument baseline or irreproducibility in thermal gradients may affect the obtained results significantly. Following an extensive experimentation we found that the "middle-sized" particle size fractions seem to be most suitable for the relaxation measurements of the chalcogenide glasses included in this study. As the structural relaxation is a purely voluminal effect, finely ground powders seemed to be overly affected by the surface defects and mechanical stress introduced into the glass grains, which together with the difficult manipulation and

increased chance for powder accumulation associated with poor heat transfer resulted in lower reproducibility. On the other hand, in the case of bulk samples the measurements were clearly influenced by increased thermal gradients within the sample even at low heating rates. The two most suitable particle size fractions with very well reproducible results and negligible affection by thermal gradients were found to be 125-180 μm and 180-250 μm. Thin layer of the powder was spread on the bottom of aluminum pan to further improve thermal contact. Masses of the samples varied between 9 and10 mg.

Regarding the specific thermal histories, two types of non-isothermal three-step cyclic relaxation experiments were applied within the framework of this article — the so called "classic" and "intrinsic" cycles. In the first step of both cycle types the sample is annealed at a temperature well above T_g to erase any previous thermal history. In the second step the sample is cooled to a temperature well below T_g at a defined cooling rate q^-, which varies within one set of the cycles from 1 to 20 K min^{-1}. In the third step the sample is subsequently heated through T_g to the initial temperature. The difference between the two types of cyclic experiments lies in the fact that while during classic cycles the heating rate is constant $q^+ = 10$ K min^{-1}, in the case of intrinsic cycles the sample is heated at the same rate at which it was previously cooled, i.e., $q^+ = |q^-|$. Each set of was performed using the same sample which was not removed from the measuring DSC cell for the whole duration of the given set. This was done in order to reduce the experimental error resulting from slightly different positioning of the sample pan in the cell. The baseline was checked before and after each set of measurements.

Cold Crystallization

In the case of studying of the crystallization behaviour, reproducibility is also one of the most important factors influencing the reliability of final results and conclusions. However, as the macroscopic crystallization process deeply depends on the actual involved crystallization mechanism — surface versus bulk — the particle size dependent study provides in this case an extensive amount of additional information on crystallization kinetics or even engaged molecular processes. Therefore, it is advantageous to perform such study while attempting to account for all involved changes in experimental conditions/thermal gradients in the interpretation of obtained results. For the purpose of this study the following powder fractions were prepared by grinding: 20-50, 50-125, 125-180, 180-250, 250-300 and 300-500 μm. In addition, also bulk samples were prepared by cracking a thin layer of as-prepared bulk glass right after its removing from the ampoule (this way of bulk samples preparation will be further referred-to in the Discussion section). Each fraction was studied separately and its kinetic analysis was performed independently. In the case of powders a thin layer of particles was

spread on the bottom of aluminum pans to improve thermal contact and at the same time to minimize the variety of the heat transfer processes (crucible-to-glass; glass-to-glass; air-to-glass — with the former being the ideal and desired one). By a very careful manipulation with sealed crucibles during their transfer to the DSC it was assured that an evenly distributed thin layer of particles is truly measured, and no irreproducible thermal gradients are produced by, e.g., cumulating or piling of the powder at the crucible wall. The distribution of the powder was always checked after each measurement when the crucible was carefully unsealed. For further improving of measurements reproducibility the crucibles with pin were used in case of all measurements in order to precise their positioning in the DSC cell. Masses of the powder samples varied in-between 9-10 mg; bulk sample masses were approximately 30 mg.

Regarding the specific DSC temperature program, it was found that Se-rich glasses from the Se-Te system have a relatively narrow distribution of relaxation times due to which the structural relaxation phenomena develop into a large overshoot effect at T_g during the heating of the material. In the case of an as-prepared or well relaxed $Se_{70}Te_{30}$ glass this overshoot tends to partially overlap with the closely following crystallization peak, which is of course highly undesirable. For this reason, each sample was first shortly annealed at a temperature just above T_g in order to erase previous thermal history and obtain a reproducibly attainable structure of undercooled liquid. This annealing may also have served as a pre-nucleation period, which will be discussed later. In the second step of the temperature program the sample was cooled at defined cooling rate of –10 K min^{-1} to 20 °C and then immediately in the last step heated up to 180 °C. The introduced procedure (initial erasing of thermal history and subsequent defined and relatively fast cooling) resulted in very small relaxation overshoot effects which no longer influenced or interfered with the crystallization process. The heating rates applied in the measuring scan (the last/third step) were: 1, 2, 3, 5, 7, 10, 15, 20 and 30 K min^{-1}. Each measurement was reproduced twice in order to estimate experimental errors.

However, before the very evaluation of kinetic analysis may be performed, one more question has to be solved – namely that of the correct data acquisition. This above all involves the problem of proper baseline subtraction. Generally, there is no reason for the heat capacities of undercooled liquid and crystal (and in consequent implication for the corresponding DSC signals before and after the crystallization peak) to be similar. However, usually the difference is very small and can be neglected – simple linear extrapolation is commonly used in this instance. Nevertheless, in the case of materials for which the aforementioned difference is not negligible (also the case of the glasses studied within the framework of this article) a proper substitution for the heat capacity transition has to be chosen. This choice is usually limited by the possibilities offered by the DSC software, as the manual programming, testing and applying several types of

extrapolations to a number of experimental curves is extremely tedious and time-demanding. Regarding the particular baseline types, besides the most common linear extrapolation, among the most widely used baselines belong various tangentially or horizontally integrated curves, splines or low-order polynomials. Several rigorous derivations concerning the thermal inertia effects are shown in, e.g., Refs [28,30]. Nonetheless, in practice it is still a matter of opinion to decide which function best simulates the thermal background under the measured kinetic effect. In our work we decided to use the cubic spline as the most appropriate baseline. As was already mentioned before, the linear baseline would be for the particular glass studied within the framework of this article inconvenient. Horizontal integration would naturally require either another prior subtraction of a defined theoretical function or a perfectly flat horizontal backgrounds at peak tails, neither of which was this case. Regarding the integrated tangents, this type of baseline is probably the second best option of those listed above, however, in the case of the undercooled liquid and crystal heat capacities both being considerably temperature dependent the spline gives better results according to our experience. And finally, splines are for interpolations usually superior to polynomials due to avoiding Runge's phenomenon [31]. As in the case of all methods that include internal calculation of the tangential slope, it is also for the spline utilization extremely important to correctly choose the data interval in for which the initial tangent will be determined. With respect to the previous, the calculated spline baseline was always carefully checked to precisely imitate the background along the considered crystallization effect in a sufficiently large temperature range.

Concerning the data acquisition, one more issue related to the extremely fast evolution of heat in the case of $Se_{70}Te_{30}$ bulk samples had to be solved. For the calculation of crystallization kinetics the actual shape of the peak is crucial; therefore, it is not sufficient to evaluate just the onset, maximum of the peak, or the amount of enthalpy corresponding to the measured effect. This is, in particular, an issue in the case of complex or competing processes where only one of the involved mechanisms is fast while the heat associated with the second (underlying) mechanism evolves slowly. In such case one can be not only limited by the factual minimum sampling interval of the DSC device (in order to obtain enough experimental points along the sharply evolving crystallization peak) but also a problem of equal distribution of the experimental data comes into question. In other words, if the experimental data are read equidistantly along the temperature axis, the ratio between experimental points present in peak tails and those present in the actual body of the peak may be unfavorable (bearing in mind that peak tails are largely influenced by the DSC device artifacts and baseline imperfections and, therefore, it is at least for the purposes of curve-fitting desirable for the most experimental data to come from the body of the peak). For this reason, an algorithm for nonlinear acquisition of experimental data was developed — equidistant readings along the course of the curve were applied. In this way each

segment of the crystallization peak has its fitting weighing factor proportional to the actual amount of evolved heat.

It was found and can be concluded that, when applying all the above mentioned procedures and conditions, nearly perfect reproducibility of the experimental data was achieved. Based on this fact, further studies of influences of various experimental conditions were possible.

Results and Discussion

This chapter will be again divided into two parts — the first dealing with structural relaxation and the second aimed at crystallization kinetics results. In both subchapters an insight into possibilities offered by interpretation of modern kinetic analysis of DSC data will be presented. Accent will be put on ideas associating the actual shape of DSC curves with molecular mechanisms while recognizing and separating the influence of thermal gradients and other data-deforming effects. In addition, several secondary objectives further outlining current authors' interests and ideas in this field will be discussed.

Structural Relaxation

The Tool–Narayanaswamy–Moynihan parameters were evaluated for the studied glasses from the Se-Te system by fitting the experimental data from both, classic and intrinsic cycles by the theoretical model. The results together with TNM parameters for pure glassy selenium [32] are presented in Table I. Graphical representation of the TNM parameters evolution with increasing Te content is given in Fig. 3. An interesting discussion of the displayed trends can be conducted based on the interpretation of the structural changes arising from the replacement of Se atoms by the Te ones (the structure of Se-Te glasses consists of heteropolar twofold coordinated helical chains and rings, where the selenium atoms are being more or less randomly replaced by the tellurium ones [33-35], several recent results [36-38] suggest that the randomness is only partial and the Te-Se bonds are prioritized over the Te-Te and Se-Se bonds). Nevertheless, before discussing the particular correlations, the authors would like to emphasize that TNM is a phenomenological model and any molecular interpretations of its parameters are unavoidably made at some risk.

As it can be seen from Fig. 3, apparent activation energy of structural relaxation Δh^* continually decreases with increasing Te content for all the studied glasses. As the incorporation of Te atoms into the selenium chains consists of a simple replacement of selenium atoms preserving the same twofold coordination, the fraction of crosslinked chains probably remains practically the same as in pure

Table I Tool–Narayanaswamy–Moynihan parameters obtained for the studied Se-Te glasses from curve-fitting of enthalpy relaxation data and from the non-fitting evaluation of classic and intrinsic cycles

	curve-fitting				non-fitting	
	$\Delta h^*/R$ kK	$\ln A$ s	$\ln x$	$\ln \beta$	$\Delta h^*_{intr}/R$` kK	$\Delta h^*_{class}/R$ kK
Se [32]	42.8 ± 0.2	–133 ± 0.5	0.52 ± 0.05	0.65 ± 0.05	43 ± 1	54 ± 2
$Se_{90}Te_{10}$	38 ± 1	–113 ± 2	0.50 ± 0.04	0.83 ± 0.03	40 ± 2	44 ± 1.5
$Se_{80}Te_{20}$	36 ± 1	–106 ± 3	0.45 ± 0.05	0.81 ± 0.05	37 ± 1.5	41 ± 1.5
$Se_{70}Te_{30}$	34.5 ± 1	–100 ± 3	0.43 ± 0.03	0.73 ± 0.02	36 ± 1	37 ± 1

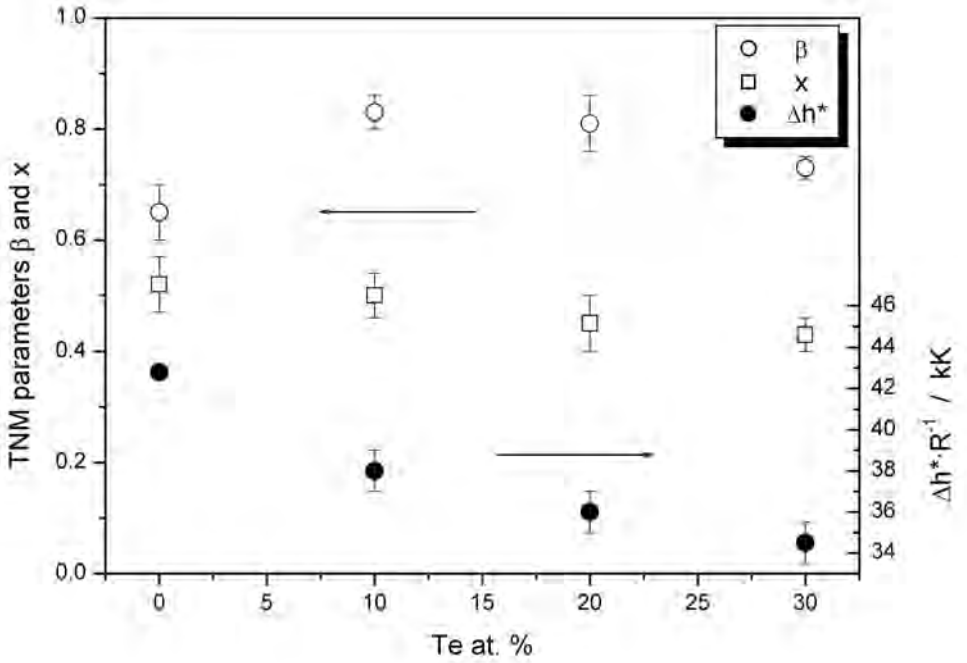

Fig. 3 Evolution of TNM parameters obtained from curve-fitting with increasing tellurium content in the Se-Te glassy system. Apparent activation energy of structural relaxation is displayed in its reduced form $\Delta h^*/R$ on a separate axis

Se. Anyway, the important fact is that no new "preset" structural units (as, e.g., the $GeSe_4$ tetrahedra in Ge-Se glasses), that would cause the structure to become heavily crosslinked or interconnected, are being formed, the consequence of which is that no initial rapid increase of activation energies with increasing Te content had to be expected. The factual decrease in Δh^* is probably related to the lower energy of Se-Te bonds [39,40]. The process of structural relaxation involves many different subprocesses (as, e.g., translation of atoms, molecules or even larger structural units, distortion of bonding angles and lengths, destruction of old bonds and formation of new ones, *etc*. — exact nature of these subprocesses is of course

dependent on specific structure of each glass), where each of them contributes to the total (macroscopic) apparent activation energy of relaxation. We believe that in the case of glasses studied within the framework of this article it is the increasing number of weaker Se-Te bonds that significantly lowers the apparent activation energy with increasing tellurium content in the glass. It was further shown by several authors [41,42] that with addition of tellurium into a glassy selenium matrix the intra-chain forces decrease while interchain forces increase. This not only supports the idea of Δh^* decreasing due to the higher content of weaker Se-Te bonds but also gives us a better picture of the very nature of relaxation processes. Decreasing apparent activation energy with increasing Te content thus implies that primary processes involved in structural relaxation of the polymeric Se matrix are based on local destruction and re-formation of interatomic bonds rather than large changes in chain conformations with only insignificant fraction of breaking bonds (which would, on the contrary, result in an increase in Δh^* due to the need for interruption of larger number of stronger van der Waals inter-chain bonds). The rate of Δh^* decrease approximately corresponds to an exponential decay function, where the initial addition of tellurium lowers the activation energy by the largest amount in comparison with the consecutive additions. Provided that glass transition temperature of pure selenium is approximately 39 °C [32], it was found that up to 30 at. % T_g increases linearly with tellurium content. Bearing in mind the evolution of apparent activation energy, it is evident that the rise in T_g cannot be due to a change in activation energy Δh^* but rather due to the change in pre-exponential factor A. From a structural point of view the increase of T_g can be accounted for by an increase in the average molar mass M_{av}, by the inclusion of heavier tellurium atoms in the polymeric Se-Te chains. The dependence of T_g on M_{av} is very well known for polymers [43,44].

The second discussed parameter of the Tool–Narayanaswamy–Moynihan model will be the non-exponentiality parameter β. This parameter is usually explained as a reflection of the width of distribution of relaxation times or as a direct measure of the deviation from the exponential decay function (which applies to single relaxation time). Though the description is mathematically equivalent, there are two different ways how a change of β is usually interpreted – each with its own physical emphasis. One way how to explain a change in the width of distribution of relaxation times is to consider varying involvement of physically distinct processes corresponding to different relaxation time components. The second, more generalized approach simply interprets β in terms of a degree of segmental cooperativity during the relaxation process. Looking at the development of the non-exponentiality in the Se-Te system, the first interesting thing to state is that the course of this dependence is not monotonic, showing a relatively large increase in β between the 0 and 10 % of tellurium content. Unfortunately, at this moment we have no additional data to reveal the steepness of this change, which

might help to identify its underlying cause. The increase in β means a narrower distribution of relaxation times, i.e., lower spatial heterogeneity. One possible explanation for this might lie in gradual initial (with respect to the increasing Te content) saturation of a number of weaker bonds engaged in the relaxation process. In other words, the lowered activation enthalpy per relaxing cluster due to the increased number of weaker Se-Te bonds may also imply a decreased degree of cooperativity (high β) and lower number of chain segments involved in the relaxation process. The suggested idea of saturation then reflects the fact that for chain-like materials the bond-breaking processes represent only a part of the relaxation event, and there is a limited number of bonds that actually break and/or are being formed again during the relaxation process. This idea is also consistent with the exponential decrease in apparent activation energy for increasing Te content. However, the ongoing replacement of stronger Se-Se bonds by weaker Te-Se bonds alone would not explain the decrease in the β parameter after the assumed saturation. Therefore, we believe that there are in fact two overlapping influences, where the second one outweighs the former after the tellurium content in the Se-Te glass is high enough to saturate the number of broken bonds during the relaxation event. True physical nature of this second effect remains, however, unclear. Increased cooperativity as a result of potentially increasing chain lengths would be inconsistent with decreasing apparent activation energy. Involvement of a brand-new relaxation process is also unlikely as the structure of the glass remains after the addition of Te atoms typologically the same. Among possible explanations might count a distortion of original selenium structure due to the integration of tellurium atoms resulting in larger spatial heterogeneity caused by the accumulation of Te atoms in certain chains, or a slowly increasing cooperativity due to the larger fraction of chains being interconnected by the van der Waals bonds [41,42]. Nevertheless, the true origin of the development of relaxation times distribution will probably remain unrecognized until very precise in-situ measurements of glassy structures on atomic level are available.

Last TNM parameter to discuss is the non-linearity parameter x. As can be seen in Fig. 3, the development of this parameter with increasing Te content may be described as a slow and roughly linear decrease. The non-linearity parameter is a measure of relative importance of macroscopic structure (defined by T_f) and temperature in determining the average relaxation time. Accordingly, with rising Te content in the Se-Te glass the importance of temperature for the very relaxation processes decreases while the importance of actual glassy structure increases. One possible explanation might again be related to the idea of apparent activation energy of structural relaxation decreasing with larger amount of weaker Se-Te bonds. As the TNM model takes into account only single averaged value of activation energy with respect to all involved subprocesses (macroscopic representation of the relaxation process), the interpretation of Δh^* decreasing primarily due to the thermodynamic structural aspects naturally implies an increase

in the relative importance of the relaxation dynamics — which is reflected in the decreasing nonlinearity parameter.

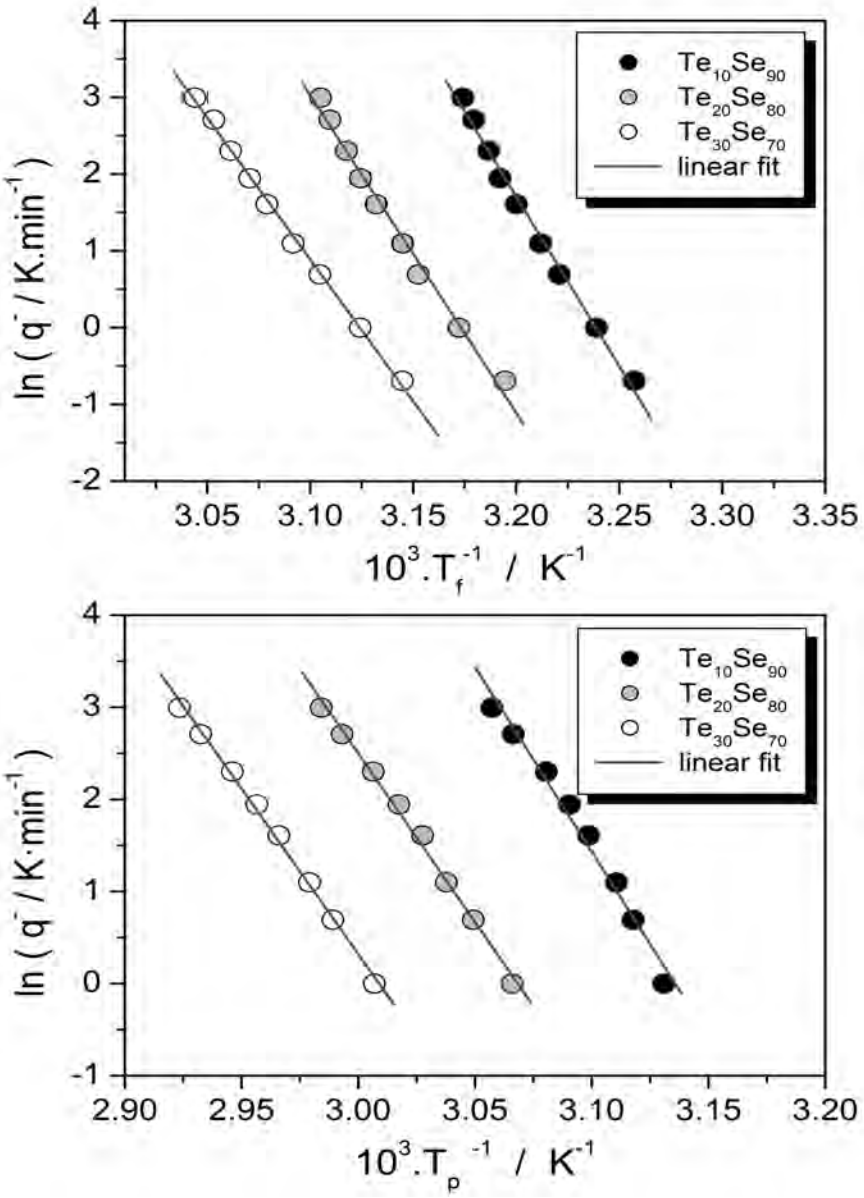

Fig. 4 Estimation of the apparent activation energy of structural relaxation $\Delta h^*/R$ from enthalpic classic (upper graph) and intrinsic (lower graph) cycles performed on all the studied glasses. Each experimental point is taken as a mean value of three measurements, experimental errors are of the magnitude of the points

Probably the most important TNM parameter concerning both, importance of physical interpretation and correctness of the curve-fitting procedure, is the apparent activation energy Δh^*. In this regard it is very important to determine this value properly and, if possible, to verify it independently too. For this reason, several non-fitting methods were derived in the past — the most famous probably being the determination of Δh^* from the dependence of T_g on cooling rate and the determination of Δh^* on the basis of peak-shift method (theoretical background can be found in the corresponding part of Theory chapter). The evaluations according

both these methods are for all three studied glasses presented in Fig. 4. All the experiments (classic and intrinsic cycle sets) were performed three times, experimental error of T_f or T_p evaluation is of the magnitude of the points if not shown otherwise. The determined values of $\Delta h^*/R$ are listed in Table I and are fairly similar to those evaluated by curve-fitting technique. It has to be noted that raw T_p values (determined from the original DSC signal) were used for the evaluation, no further correction for the influence of heating rate (as suggested, e.g., in Ref. [45]) was made. The need for correction might possibly come into question in the case of $Se_{90}Te_{10}$, where there is an apparent curvature in the $\ln(q^-)$-T_p^{-1} dependence and the correction might actually improve accuracy of the determined Δh^* value. However, in our work no further results are derived from the Δh^*_{intr} and the very value is used just for an estimative comparison, therefore we took the liberty to show an evaluation of the raw DSC data in order to emphasize this often neglected inaccuracy. The determined values of $\Delta h^*/R$ are in the case of the method based on dependence of T_g on cooling rate slightly higher than those evaluated by curve-fitting technique, which may be caused by the uncertainty of the T_f determination or by the temperature gradients and resulting deviations of the sample temperature from the programmed one.

In conclusion it can be said that under the premise of a very careful and precise experiment conduction very interesting outcomes may be derived based on the evolution of TNM parameters with glass composition. The keystone is, of course, precise identification and separation of the relaxing structure manifestations from measurement artifacts caused by unideal experimental conditions.

Cold Crystallization

As in the case of structural relaxation kinetics, also for crystallization evaluations probably the most important parameter, by which all consequent calculations are driven and kind of determined, is the apparent activation energy of the process. In our work the Kissinger [17] and Friedman [18] methods already described in the Theory part — Eqs. (10) and (11) — were used for determination of E_A. The results obtained by applying the two aforementioned methods to the experimental data are listed in the Table II for all three studied chalcogenide glasses and all prepared fractions. Graphical representation of the Kissinger method results is then given in Fig. 5. The particle size fractions were distributed according to the average particle size; the value of 1 mm was assigned to the bulk specimen. The Friedman method was omitted from the figure for the clarification as both methods provide fairly similar values of E_A anyway. The only exception from this consistency were the bulk values. It was already mentioned earlier that in the case of $Se_{70}Te_{30}$ bulk samples an extremely fast and extensive evolution of heat took place, which due to the large thermal gradients and resulting lags significantly deformed the crystal-

Table II Activation energies evaluated by Kissinger and Friedman methods and values of a kinetic parameter *mJMA* determined according to Málek and Šesták for all particle size fractions of the studied Se-Te glasses

Sample size mm	$E_{Kissinger}$ kJ mol^{-1}	$E_{Friedman}$ kJ mol^{-1}	m_{Malek}	m_{Sestak}	ln(A/s)
$Se_{90}Te_{10}$					
0.020-0.050	124±3	117±6	1.2±0.5	1.5±0.3	34.7±0.1
0.050-0.125	106±4	106±3	2.1±0.4	2.4±0.5	28.1±0.1
0.125-0.180	103±3	107±2	2.0±0.2	2.6±0.6	26.9±0.1
0.180-0.250	98±3	92±4	1.7±0.3	2.5±0.7	25.2±0.2
0.250-0.300	95±4	70±5	1.4±0.1	1.7±0.3	24.0±0.2
0.300-0.500	93±6	95±4	1.3±0.1	1.5±0.2	23.4±0.8
Bulk	86±3	-	7±13	2.8±0.3	23.0±0.4
$Se_{80}Te_{20}$					
0.020-0.050	124±2	123±2	1.4±0.1	1.7±0.2	33.5±0.1
0.050-0.125	116±1	117±1	1.3±0.1	1.5±0.1	30.2±0.1
0.125-0.180	109±2	115±3	1.3±0.1	1.6±0.2	27.7±0.2
0.180-0.250	112±2	109±3	1.2±0.1	1.5±0.1	27.9±0.1
0.250-0.300	109±2	104±4	1.2±0.1	1.5±0.1	27.0±0.1
0.300-0.500	109±3	101±3	3.6±1.1	1.7±0.2	26.9±0.2
Bulk	99±6	112±4	12±10	3.6±0.9	23.4±0.2
$Se_{70}Te_{30}$					
0.020-0.050	158±2	150±3	1.1±0.1	1.3±0.1	45.5±1.2
0.050-0.125	147±2	141±5	1.1±0.1	1.3±0.1	41.4±1.1
0.125-0.180	135±2	128±6	1.4±0.5	1.4±0.1	37.8±0.8
0.180-0.250	127±2	120±5	3.0±1.5	1.5±0.2	34.7±1.1
0.250-0.300	125±1	117±5	5.4±4.1	1.6±0.1	32.5±0.1
0.300-0.500	121±1	113±3	7.8±4.8	1.5±0.1	31.5±0.1
Bulk	114±3	148±8	4.4±3.2	5.1±0.8	30.3±0.4

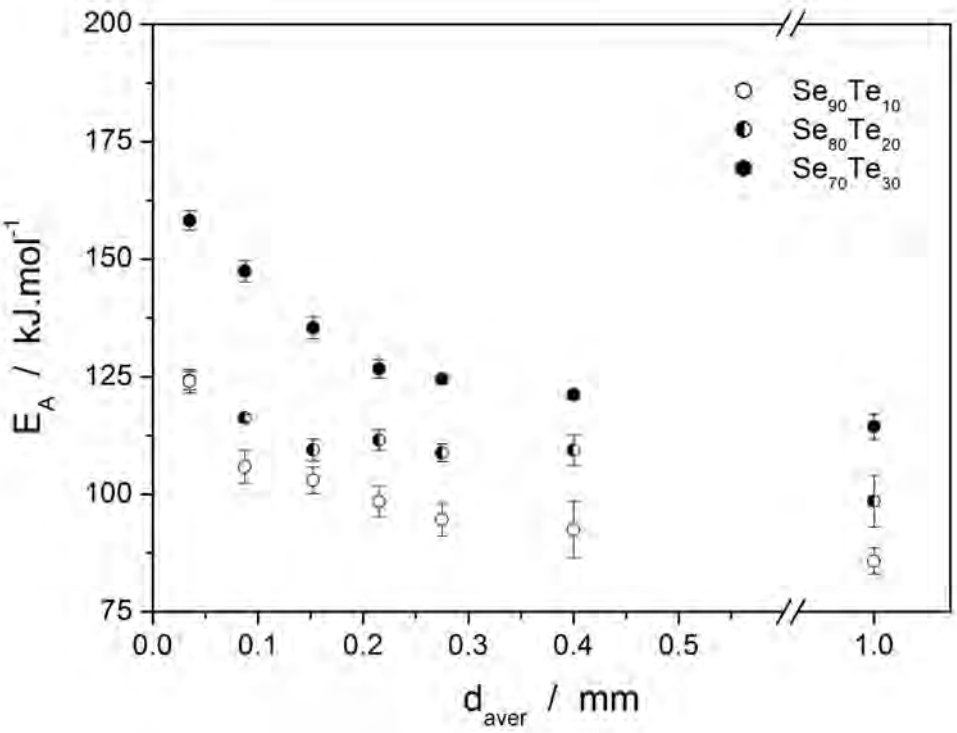

Fig. 5 Comparison of apparent activation energies determined for all three studied Se-Te glasses according to Kissinger in dependence on average particle size in particular fractions. Bulk samples were assigned d_{aver} = 1 mm

lization peak at higher heating rates. The other two compositions, on the other hand, did not suffer from this effect, however, another complication occurred – namely the tendency for separation of the two involved crystallization mechanisms, which in the case of bulk specimens resulted already in largely pronounced shoulders deforming the peak completely. Similar issue occurred, of course, also in the case of some other high-particle-size fractions but only for few "extreme" heating rates, which were consequently excluded from the $E_{A,iso}$ determination. The main point of this discussion pointed at the Friedman method is then a suggestion not to overrate its potency. One should always bear in mind that if applied blindly, the isoconversional methods may in certain cases provide biased and unrealistic results due to the natural dependence of these methods on evaluation of α based solely on mathematical computation. Unlike the Kissinger method, where the determination of E is given by the actual physical essence of the crystallization process (the maximum of the heat evolution rate is driven entirely by the fundamental crystallization mechanism), which in addition is almost independent of the experimental conditions, the evaluation according to the Friedman method is heavily dependent on the actual shape of the peak (due to the purely mathematical calculation of α) and, therefore, correspondingly, the results of this method may be largely influenced by every possible change in experimental conditions that can occur either with the change of heating rate or simply with the long-term duration of the experiments sequence.

Nevertheless, if we look back at the Fig. 5, several conclusions can be

drawn. It can be seen that the activation energy of the crystallization process E_A increases with rising tellurium content. This is in a perfect agreement with what is known about selenium and tellurium molecular structures [1,46]. Namely the inter-chain distances are in the case of tellurium significantly shorter than in selenium and delocalized bonds causing quasi-metallic conductivity are formed between the tellurium chains. In consequence, these bonds are most probably the reason for the crystallization activation energy increasing with higher tellurium content. In addition, the inter-chain bonding causes the material to react more homogeneously, which may be the corroborative argument for the faster tellurim-responsible internal crystallization (as will be shown later). Second conclusion derived from what is apparent in Fig. 5 is related to the very particle size dependencies of E_A. It can be seen that for all three studied glasses the apparent activation energy at first steeply decreases with increased glass grain size and then sort of limits towards the value assigned to bulk sample. This is in a perfect agreement with the fact that two crystallization mechanisms (surface and bulk) are involved in the overall process, where the surface crystallization has considerably higher activation energy. As the ratio of the involvement of the two mechanisms changes (due to decreasing number of surface defects and dislocations and increasing "amount" of bulk material potentially containing/available for creation of volume nuclei) the averaged activation energy also follows monotonous convergent trend. The important term in previous sentence is the word "averaged", which is closely associated with the actual nature of intercoupling between the two mechanisms.

The second block of thoughts and comments in the Cold crystallization subchapter will be intent on the question of determination of the prevailing/dominant crystallization mechanism. A very thorough paper on this topic was published by Ray and Day [47], who established several basic criteria (Φ_p – heat flow corresponding to the maximum of the peak, i.e., the maximum peak height; ΔT_{hh} – half-width of the peak, i.e., the width of the peak in the half of its height) and from the course of their dependence when plotted against the average particle size they decided whether the dominant crystallization mechanism is associated with surface defects and dislocations rather than with bulk nuclei. Although the criteria introduced by Ray and Day are very simple and relatively easy to evaluate, we would like to introduce in this article a new (to the authors' knowledge original) criterion that is also extremely simple to apply but, in addition, it is independent of the most negative influences of experimental conditions (like those of, e.g., thermal gradients arising from the arrangement of the DSC cell itself or gradients associated with the unideal thermal contact of particular sample grains with the bottom of DSC crucible) due to the only monitored quantity being T_p, which is (as already discussed earlier) from the considered point of view a very robust value to determine. This method is, in fact, based on the very essence of the idea of joint influence of bulk and surface crystallization mechanisms. The influence of the prevailing mechanism obviously determines/drives the

crystallization process and takes control over it already at moderate amounts of either surface defects and dislocations (in the case of surface crystallization) or bulk nuclei (in the case of volume crystallization). On the other hand, correspondingly, the number of preferred crystallization centres has to be very small in order for the secondary crystallization mechanism to dominate.

Implication of this fact can be well demonstrated by help of Fig. 6, where the Kissinger plots for the three studied glasses are compared. It is well apparent that in the case of $Se_{70}Te_{30}$ the dependencies sort of "limit" to the one mostly influenced by the driving mechanism — volume/bulk crystallization is dominant in this glass. Similar but not so pronounced limitation is also apparent in the case of the $Se_{80}Te_{20}$ glass, where the bulk crystallization is also still present in a large extent. On the other hand, the plot for the $Se_{90}Te_{10}$ glass, where the intensities of surface and bulk crystallization mechanisms are comparable, does not show any limitation whatsoever. In order to quantify this phenomenon, it is suitable to plot the value of the temperature corresponding to the maximum of the crystallization peak T_p in dependence on the logarithm of the average particle size present in the respective fraction $\ln(d_{aver})$ — see the right column in Fig. 6. In this depiction the dependence limits towards either bulk or fine powder values accordingly with the dominant crystallization mechanism. The conclusions resulting from this way of depiction are more definite and clear in comparison with the left-side Kissinger-plot-type of evaluation. In the case of $Se_{70}Te_{30}$ glass the dependence unambiguously limits to the bulk value, thus volume crystallization mechanism clearly dominates; for $Se_{80}Te_{20}$ glass where surface crystallization manifests to a larger extent no prevailing limitation is apparent due to both mechanisms being considerably overlaid in case of all particle size fractions and heating rates; and finally for the $Se_{90}Te_{10}$ glass with the surface crystallization starting to dominate the dependence is all but limiting towards bulk value. The dependence for the $Se_{90}Te_{10}$ glass cannot be, however, described as limiting to the fine powders values (indicating fully dominant surface crystallization as does similar dependence in the case of, e.g., $Ge_2Sb_2Se_5$ glass [48]), which has to be interpreted in terms of both the mechanisms still competing and manifesting themselves at comparable levels. All above mentioned conclusions derived on the basis of the newly introduced method were confirmed by applying the criteria developed by Ray and Day [47], which gave similar, yet not so straightaway, outcomes.

The following paragraphs are going to be describing in the authors' opinion probably the most interesting part of the crystallization kinetic analysis presented in this article — i.e., the interpretation of the characteristic $z(\alpha)$ and $y(\alpha)$ functions (Eqs (12) and (13) — see the Theory part). Primarily, reason for this particular transformation of experimental data is to determine an appropriate kinetic model and to estimate the value of its parameter based on the values of $\alpha_{max,z}$ and $\alpha_{max,y}$ (the values of α corresponding to the maxima of the respective functions). However, in the following text we would like to demonstrate that the characteristic

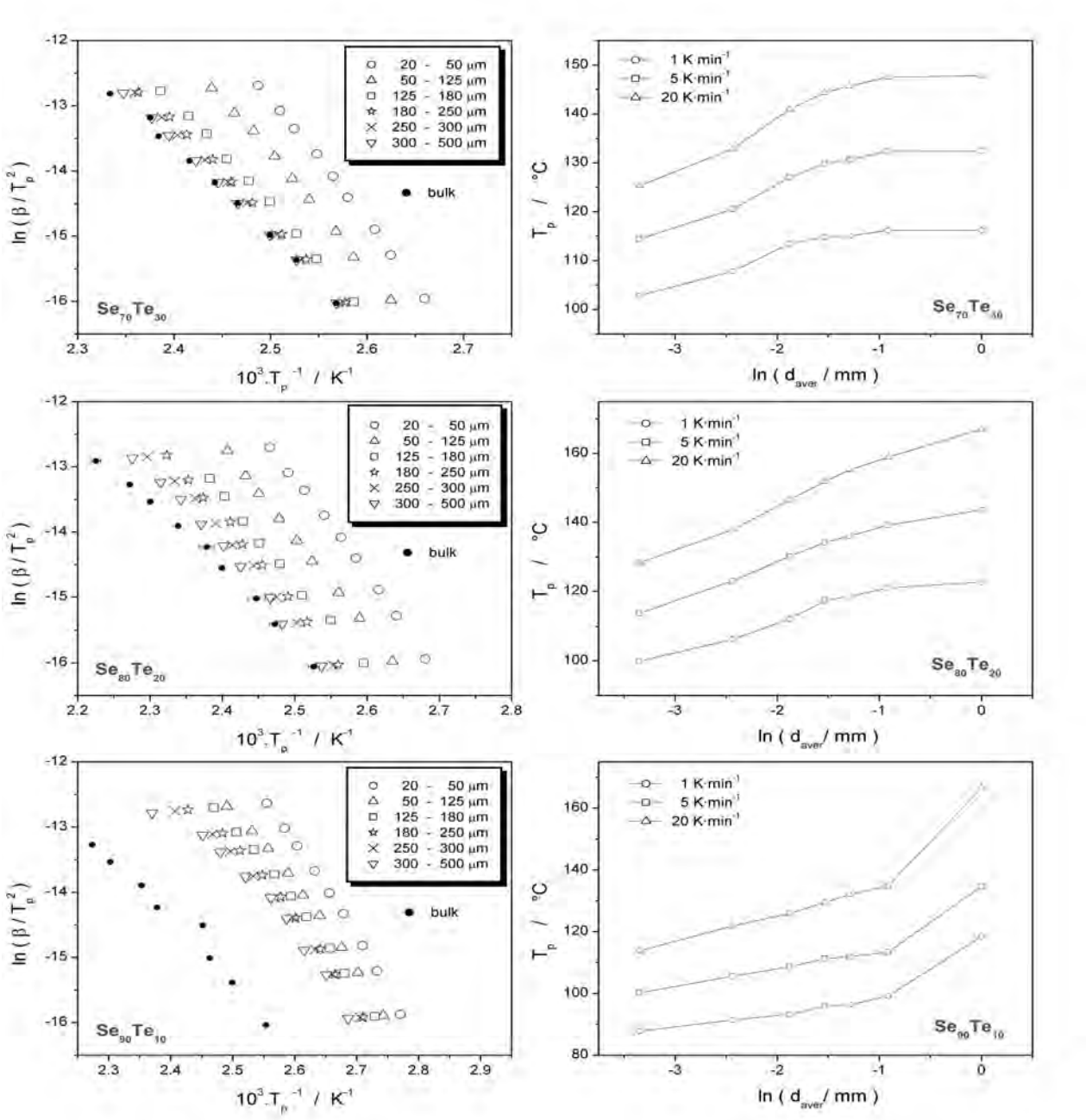

Fig. 6 Left column – comparison of Kissinger plots for a set of particle size fractions measured for the three studied Se-Te chalcogenide glasses. Right column – normalized crystallization mechanism plots introduced in this work in order to determine the dominating crystallization mechanism. See text for details

functions actually provide a lot more additional information if compared in dependence on particle size and composition.

The most interesting and pronounced behaviour in terms of change in crystallization kinetics is observed in the $Se_{70}Te_{30}$ glass. Therefore this composition will be discussed in the largest detail, the other two studied glasses will then only be commented regarding the changes with respect to the $Se_{70}Te_{30}$ glass. Figure 7 shows characteristic kinetic functions $z(\alpha)$ and $y(\alpha)$ for three chosen particle size fractions of the $Se_{70}Te_{30}$ glass (each row corresponds to one particular fraction).

The chosen fractions represent gradual trend in the dependence of crystallization kinetics on particle size. Looking first at the $z(\alpha)$ functions it can be seen that their maximum at least roughly corresponds to the value typical for the JMA model (see algorithm in Fig. 2, theoretical value for this model is 0.632). It can further be seen that the $z(\alpha)$ functions are completely invariant with respect to the applied heating rate and other experimental conditions. These conclusions both suggest and confirm applicability of the JMA model. On the other hand, the course of $y(\alpha)$ functions clearly shows several significant dependencies. The most evident trend in the course of $y(\alpha)$ functions is the shift of their maximum towards higher values of α with increasing particle size. As was already shown in the previous block of comments, the prevailing/dominant crystallization mechanism in $Se_{70}Te_{30}$ glass is associated with the bulk processes. Nevertheless, the maximum of the $y(\alpha)$ function corresponding to the finest particle size fractions clearly indicates the JMA kinetic exponent $m = 1$ ($\alpha_{max,y} \sim 0$; linear decrease), which is usually attributed to the surface crystallization mechanism. However, with the increasing particle size this surface mechanism recedes and the second y(α) "peak" arises with $\alpha_{max,y}$ equal to approximately 0.5- 0.6 corresponding to the bulk crystallization mechanism. This interpretation is perfectly consistent with the idea of both crystallization mechanisms (surface and bulk) being present, where the intensity/representation of each particular process is given by the ratio of the number of surface defects or dislocations to volume nuclei, i.e., for the finest fractions, where during the grinding procedure a large number of surface defects acting like crystallization centres was created and, moreover, the actual surface area was significantly increased, the prevailing mechanism is the surface crystallization. On the other hand, in the case of coarse fractions the grinding was not so intensive (not applied at all in the case of bulk), the result of which was low amount of surface defects and a much more favorable ratio of the bulk/surface crystallization centres for the crystallization mechanism to be driven by the volume nucleation and continuing crystal growth. In the case of middle-sized powder fractions there are both factors present, quite large number of surface defects resulting from the grinding and sample-preparation procedures and, at the same time, relatively high number of bulk nuclei due to the glass particles having larger size. Another evidence for this interpretation is also the fact that the surface crystallization mechanism ($m_{JMA} = 1$) entirely disappears only for the bulk sample, which only was not processed in any way that could cause creation of a significant/increased number of surface defects.

The second trend visible in Fig. 7 is the shift in crystallization mechanism with the applied heating rate. It is apparent that for low heating rates the bulk mechanism is more pronounced (due to the normalization of characteristic functions in Fig. 7, this effectively looks like a depression of the surface crystallization). There are several ways how to interpret this phenomenon. In the authors' opinion the most probable one is to imply the conclusion resulting from the Fig. 5, i.e., to employ the difference in activation energies for the two crystal-

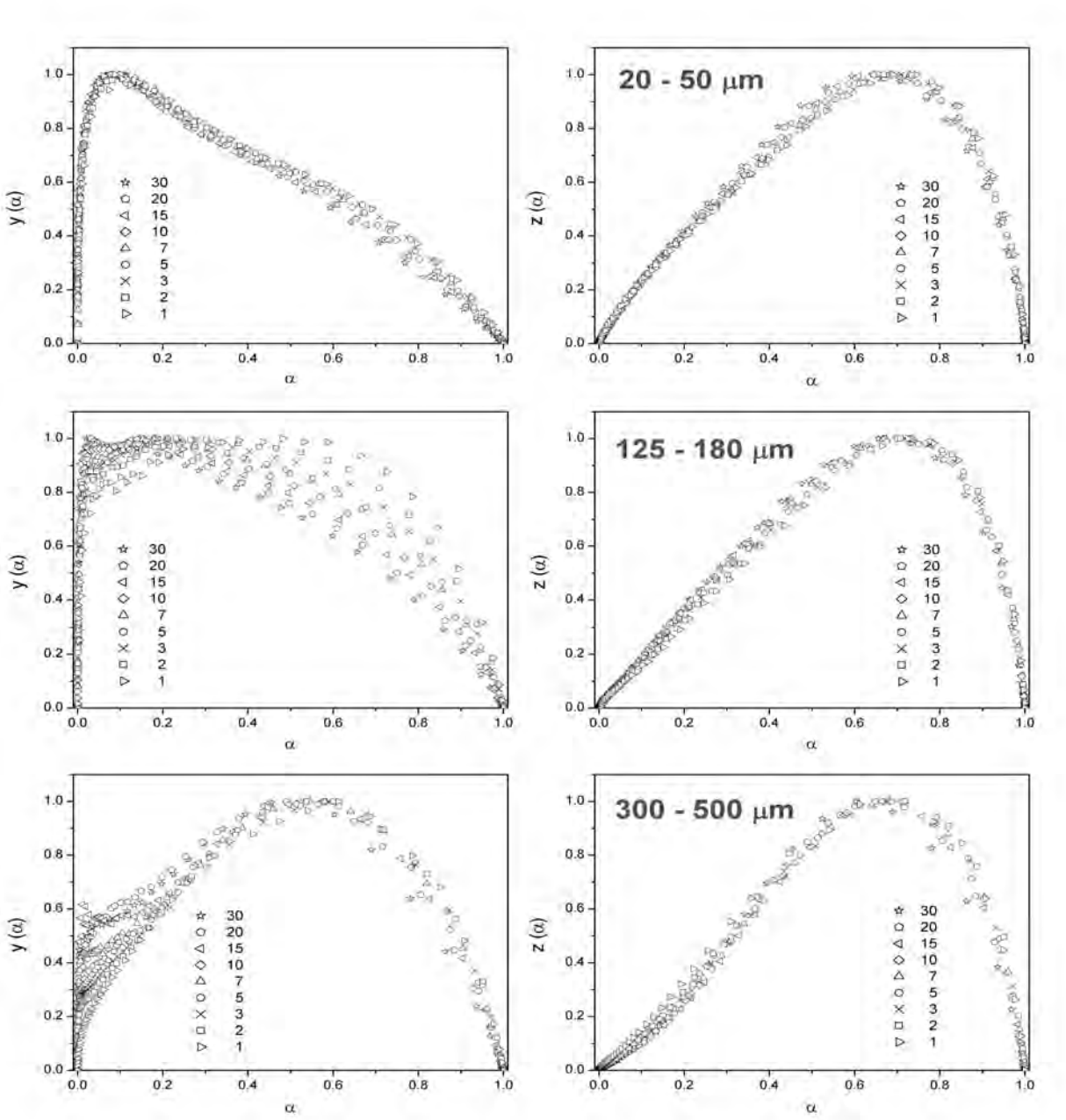

Fig. 7 Normalized $y(\alpha)$ and $z(\alpha)$ functions corresponding to non-isothermal measurements of chosen particle size fractions of $Se_{70}Te_{30}$ glass. Particular rows match the individual studied fractions

lization mechanisms into the explanation of the effect discussed in this paragraph. It is clearly apparent from Fig. 5 and Table II that the surface crystallization appears to have slightly but still significantly higher activation energy than the bulk process. On the other hand, the three-dimensional kinetics is axiomatically slower and can be further decelerated by, e.g., steric reasons. As can be seen already from Fig. 7 (and as will be proven later) the first process that takes place is always the surface crystallization that corresponds to the earliest heat evolution. Therefore during the fast heating the starting primary surface crystallization mechanism takes control over the larger partition of the complex crystallization process (with more

than enough energy being provided by the faster heating and thermal gradients causing the whole process to be allocated to higher temperatures), while the slower bulk mechanism does not have enough time to fully develop (in accordance with the concept of competing processes). Correspondingly, at low heating rates it is the difference in activation energies that determines the outcome — although it is still the surface crystallization that starts the complex crystallization, the energy input (caused by the factual temperature increase plus heat evolved during the crystallization) is relatively low and an actual competition based on the difference in energy barriers (represented by the apparent activation energy E_A) takes place causing the bulk process to be more pronounced while "consuming" larger part of the provided energy.

Similar conclusions can be drawn for the two other chalcogenide glasses studied within the framework of this research ($Se_{80}Te_{20}$ and $Se_{90}Te_{10}$). The $z(\alpha)$ functions for all studied particle size fractions of these two glasses were very consistent with regard to applied heating rate and were undoubtedly pointing to the usage of the JMA kinetic model. Certainly more interesting was the course of the $y(\alpha)$ functions. The $y(\alpha)$ characteristic kinetic functions are shown in Fig. 8 for several chosen most interesting fractions of both currently discussed glasses. In the case of $Se_{80}Te_{20}$ glass it can be seen that for the 20-50 μm and 125-180 μm fractions the $\alpha_{max,y}$ still unambiguously corresponds to the surface crystallization mechanism. In addition it can be seen that the shape of the functions is almost invariant with respect to applied heating rate. Nevertheless, in case of the 125-180 μm particle size fraction a very small shoulder can be already observed on the high-α side of the function, corresponding to the manifesting bulk crystallization mechanism. The volume crystallization then becomes fully pronounced in the case of the 300-500 μm particle size fraction, where a relatively strong dependence on the heating rate occurs. In the case of bulk sample (which is not displayed in the figure) the shape of the $y(\alpha)$ function, on the other hand, corresponded perfectly to a bulk crystallization mechanism with practically no trace of the surface shoulder. If we compare the course of $y(\alpha)$ functions for the $Se_{70}Te_{30}$ and $Se_{80}Te_{20}$ glasses, several differences are apparent. While in the case of the $Se_{70}Te_{30}$ glass the transition between the two involved mechanisms is quite distinct, in the case of the $Se_{80}Te_{20}$ glass their manifestation is kind of merged together. This is well consistent with the fact that for the $Se_{80}Te_{20}$ glass the activation energies of the two mechanisms are relatively close (opposed to the $Se_{70}Te_{30}$ glass), which apparently results in the shift along the conversion rate axis. Moreover, it can be said that in the case of $Se_{80}Te_{20}$ glass the surface crystallization mechanism becomes a lot more prominent, which is again consistent with results presented in former paragraphs. Otherwise most conclusions derived for the $Se_{70}Te_{30}$ glass are valid also in the case of the $Se_{80}Te_{20}$ glass.

The second studied material displayed in Fig. 8 is the $Se_{90}Te_{10}$ glass. Also in the case of this glass the surface crystallization mechanism is well pronounced

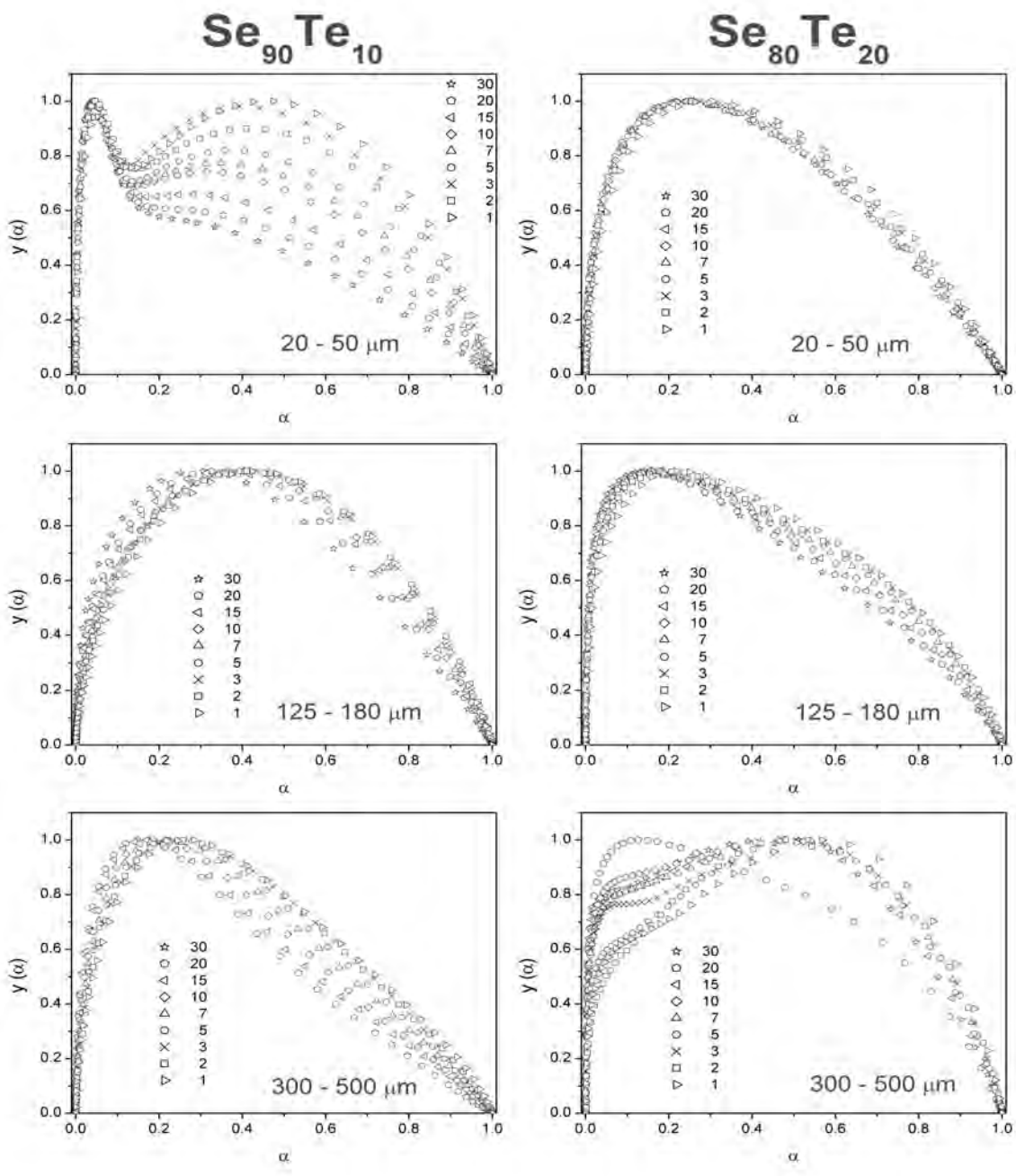

Fig. 8 Normalized $y(\alpha)$ functions corresponding to non-isothermal measurements of chosen particle size fractions of $Se_{90}Te_{10}$ and $Se_{80}Te_{20}$ glasses. Particular rows match the individual studied fractions

and, in fact, seems to become the dominant one. Nevertheless, the bulk mechanism still remains present — in the case of bulk (which is again not displayed the figure) the $y(\alpha)$ functions start to show strong dependence on heating rate similar to that displayed for the 300-500 μm fraction of $Se_{80}Te_{20}$ glass. This shift towards larger particle sizes again implicates larger portion of the surface crystallization mechanism involved. However, this is also the most probable cause of the tendency for time-axis-based separation of the two processes occurring in the extreme cases of the surface-to-bulk nuclei number ratio (the 20-50 μm and bulk fractions). This

is well apparent on the course of the $z(\alpha)$ function where in such case a shoulder appears. These conclusions again well correspond to the detailed interpretations discussed in the case of the $Se_{70}Te_{30}$ glass.

The actual results of the kinetic analysis for the three studied compositions from Se-Te glassy system studied within the framework of this research are given in Table II. The values of pre-exponential factor as well as the values of the kinetic parameter m_{JMA} were calculated as a mean value from all heating rates applied to the respective particle size fraction. The indexing in the case on the JMA model parameter corresponds to the method of evaluation — the index "Malek" denotes determination in accordance with Eq. (15) and the index "Sestak" is associated with evaluations according to Eq. (16). It can be said that while in the case of fine and middle sized particle size fractions it is the evaluation according to Málek (Eq. (15)) which provides more reasonable values (corresponding to what can be derived from the overall course in the shape of characteristic kinetic functions), in the case of coarse fractions and bulk this method provides incorrect values due to the shift of the $\alpha_{max,y}$ towards too high values (caused by the partial separation of the two involved crystallization mechanisms). In the case of these samples it is the double logarithm function (Eq. (16)) which provides correct results (or at least their reasonable estimates). However, it has to be remarked that the double logarithm function in these cases is usually not linear in the whole interval, and only the part corresponding to the dominant crystallization mechanism has to be chosen in order to obtain correct results.

Conclusion

The enthalpic relaxation of chosen compositions from the Se-Te glassy system was described on the basis of Tool–Narayanaswamy–Moynihan model. All the performed DSC measurements of respective compositions were fitted using a single set of TNM parameters. Based on the development of particular TNM parameters with increasing Te content and on the mutual comparison of the parameters, an attempt for explanation and semi-qualitative description of the relaxation features in the Se-Te glassy system was made on the basis of specific molecular structures and their changes during relaxation. In addition, two non-fitting methods of Δh^* parameter estimation were applied to our data. A good agreement between estimates and curve-fitting results was achieved for the evaluation from intrinsic cycles: the evaluation of Δh^* from classic cycles provided a slightly higher value of apparent activation energy compared to the curve-fitting.

Complete kinetic analysis of the studied glasses was performed in terms of the Johnson–Mehl–Avrami model. Complexity of the competing surface and bulk mechanisms was explained both, qualitatively and quantitatively. The obtained

DSC data allowed explaining of the mutual interaction of the processes as well as of the origin of their sequentiality. Discussion of the observed effects, shifts in temperature and deviations from ideal model behaviour was conducted on the basis of thermal gradients, surface crystallization centres arising from the sample preparation treatments and amount of volume nuclei originating from the combination of pre-nucleation period and the very glass preparation phase. The presented conclusions are thus general and qualitatively valid for all similar types of complex processes.

As a concluding remark the authors would like to note that although advanced interpretation of the DSC curves provides even in the case of complex processes answers to a number of fundamental kinetic questions, differential scanning calorimetry itself is not an ultimate technique and always should be accompanied by supplemental information about molecular structures (XRD, EXAFS etc.) and/or crystal growth kinetics (optical or electron microscopy) in order to give full and consistent picture of relaxation and crystallization behaviour in the studied material.

Acknowledgements

This work has been supported by the Grant Agency of the Czech Republic under projects No. 106/10/P035 and 106/11/1152.

References

[1] Bureau B., Boussard-Pledel C., Lucas P., Zhang X., Lucas J.: Molecules **14**, 4337 (2009).
[2] Shukla R. K., Swarup S., Kumar A., Nigam A. N.: Phys. Stat. Sol. **115**, K105 (1989).
[3] Yang H., Wang W., Min S.: J. Non-Cryst. Sol. **80**, 503 (1986).
[4] Scherer G.W.: Relaxation in Glass and Composites, Chapter 9, John Wiley & Sons, New York, 1986.
[5] Tool A.Q.: J. Am. Ceram. Soc. **29**, 240 (1946).
[6] Tribone J.J., O'Reilly J.M., Greener J.: Macromolecules **19**, 1732 (1986).
[7] Gardon R., Narayanaswamy O.S.: J. Am. Ceram. Soc. **53**, 380 (1970).
[8] Narayanaswamy O.S.: J. Am. Ceram. Soc. **54**, 491 (1971).
[9] Moynihan C.T., Easteal A.J., DeBolt M.A., Tucker J.: J. Am. Ceram. Soc. **59**, 12 (1976).
[10] Hodge I.M., Berens A.R.: Macromolecules **15**, 762 (1982).
[11] Ritland H.N.: J. Am. Ceram. Soc. **38**, 86 (1955).

[12] DeBolt M.A., Easteal A.J., Macedo P.B., Moynihan C.T.: J. Am. Ceram. Soc. **59**, 16 (1976).
[13] Hutchinson J.M., Kovacs A.J.: Polym. Eng. Sci. **24**, 1087 (1984).
[14] Hutchinson J.M., Ruddy M.: J. Polym. Sci. **B26**, 2341 (1988).
[15] Hutchinson J.M., Ruddy M.: J. Polym. Sci. **B28**, 2127 (1990).
[16] Málek J., Klikorka J.: J. Therm. Anal. **32**, 1883 (1987).
[17] Kissinger H.E.: Anal. Chem. **29**, 1702 (1957).
[18] Friedman H.L.: *Kinetics of Thermal Degradation of Char-Forming Plastics from Thermogravimetry*, Wiley Subscription Services, Inc., A Wiley Company, New York, 1964.
[19] Málek J.: Thermochimica Acta **355** 239 (2000.
[20] Málek J.: Thermochimica Acta **200**, 257 (1992).
[21] Avrami M.: J. Chem. Phys. **7**, 1103 (1939).
[22] Avrami M.: J. Chem. Phys. **7**, 212 (1940).
[23] Avrami M.: J. Chem. Phys. **7**, 177 (1941).
[24] Henderson D. .: J. Therm. Anal. **15**, 325 (1979).
[25] Henderson D.W.: J. Non-Cryst. Sol. **30**, 301 (1979).
[26] Málek J.: Thermochim. Acta **138**, 337 (1989).
[27] Málek J., Mitsuhashi T.: J. Am. Ceram. Soc. **83**, 2103 (2000).
[28] Šesták J.: *Thermophysical Properties of Solids, Their Measurements and Theoretical Analysis*, Elsevier, Amsterdam, 1984.
[29] Málek J., Criado J. M., Šesták J., Militký J.: Thermochim. Acta **153**, 429 (1989).
[30] Šesták J.: *Science of Heat and Thermophysical Studies: A Generalized Approach to Thermal Analysis*, Elsevier, Amsterdam, 2005.
[31] Runge C.: Zeitschrift für Mathematik und Physik **46**, 224 (1901).
[32] Svoboda R., Pustková P., Málek J.: J. Phys. Chem. Sol. **68**, 850 (2007).
[33] Venugopal R. K., Bhatnagar A. K.: J. Phys. D: Appl. Phys. **25**, 1810 (1992).
[34] El-Korashy A., El-Zahed H., Radwan M., Abdalla A. M.: Thin Solid Films **261** 328 (1995).
[35] Shimakawa K., Nitta S.: Phys. Rev. **B17**, 3950 (1978).
[36] Afify N., Gaber A., Abdalla I., Talaat H.: Physica **B 229** 167 (1997).
[37] Majid M., Benazeth S., Souleau C., Purans J.: Phys. Rev. **B58**, 6104 (1998).
[38] Tsuzuki T., Yao M., Endo H.: J. Phys. Soc. Jpn. **64**, 485 (1995).
[39] Nesheva D., Kotsalas I.P., Raptis C., Arsova D.: J. Appl. Phys. **86**, 4964 (1999).
[40] Kasap S.O., Juhasz C.: J. Mat. Sci. **21**, 1329 (1986).
[41] Ionov R., Dudev T.: Appl. Phys. **A55**, 203 (1992).
[42] Martin R.M., Lucovsky G., Helliwell K.: Phys. Rev. **B13**, 1383 (1976).
[43] Fox T.G., Flory P. J.: J. Polym. Sci. **14**, 315 (1954).
[44] Fox T.G., Loshaek S.: J. Polym. Sci. **15**, 371 (1955).

[45] Hutchinson J. M., Ruddy M., Wilson M. R.: Polymer **29**, 152 (1988).
[46] Bureau B., Danto S., Ma H.L., Boussard-Plédel C., Zhang X. H., Lucas J.: Solid State Sci. **10**, 427 (2008).
[47] Ray C. S., Day D. E.: Thermochim. Acta. **280281**, 163 (1996).
[48] Svoboda R., Málek J.: J. Non-Cryst. Sol. **358**, 276 (2012).